

# Microbial Ecology and Biogeography OF THE Southern Ocean

David Wilkins

October 23, 2012

# Contents

<b>List of Figures</b>	iii
<b>List of Tables</b>	v
<b>List of Acronyms</b>	vii
<b>Acknowledgements</b>	ix
<b>Abstract</b>	xi
<b>Introduction</b>	1
Microbial ecology of the Southern Ocean . . . . .	1
Oceanography of the Southern Ocean . . . . .	1
Water masses and fronts . . . . .	1
Effect of climate change . . . . .	1
Role of the Polar Front in biogeography . . . . .	1
Project questions and hypotheses . . . . .	1
<b>The Polar Front as a major biogeographic boundary in the Southern Ocean</b>	3
Summary . . . . .	3
Introduction . . . . .	3
Methods . . . . .	3
Sampling and metagenomic sequencing . . . . .	3
Phylogenetic analysis of metagenomic data . . . . .	5
Functional analysis of metagenomic data . . . . .	8
Results . . . . .	9
Metagenomic sequencing . . . . .	9
Phylogenetic analysis of metagenomic data . . . . .	10

Functional analysis of metagenomic data	14
Discussion	14
Conclusions	14
<b>Meso-scale biogeographic drivers of planktonic diversity</b>	<b>19</b>
<b>Conclusions</b>	<b>21</b>

# List of Figures

1	Map showing sites of seawater samples used in the Polar Front study . . . . .	4
2	Rank-abundance curves for OTUs in each zone and size fraction . . . . .	10
3	Contribution of Operational Taxonomic Units (OTUs) to variance between the North and South zones . . . . .	13
4	TODO master caption . . . . .	15



# List of Tables

1	Details of samples used in Polar Front study . . . . .	6
2	Twenty most abundant OTUs . . . . .	11
3	Highest-contributing OTUs to the difference between the North and South zones . . . .	12
4	Contributions of KEGG modules to variance between the North and South zones . . . .	16
5	Contributions of KEGG ortholog groups to variance between the North and South zones	17



# Acronyms

**GAAS** Genome relative Abundance and Average Size.

**GLPSOL** GLPK LINEAR PROGRAMMING/MIP SOLVER.

**ANOSIM** Analysis of SIMilarities.

**AZ** Antarctic Zone.

**CEAMARC/CASO** Collaborative East Antarctic Marine Census/Climate of Southern Ocean.

**CTD** Conductivity, Temperature and Depth.

**GLPK** GNU Linear Programming Toolkit.

**KEGG** Kyoto Encyclopedia of Genes and Genomes.

**NZ** North Zone.

**OTU** Operational Taxonomic Unit.

**PF** Polar Front.

**PFZ** Polar Frontal Zone.

**SIMPERS** SIMilarity PERcentages.

**SZ** South Zone.

**UFO** Unidentified Flying Object.



# Acknowledgements



# **Abstract**

# **Introduction**

This is a test of the acronyms: I saw a Unidentified Flying Object (UFO). It was not the first UFO I'd ever seen. In fact, I've seen 100 UFOs.

Here is some greek:  $\mu\text{g}$ .

**Microbial ecology of the Southern Ocean**

**Oceanography of the Southern Ocean**

**Water masses and fronts**

**Effect of climate change**

**Role of the Polar Front in biogeography**

**Project questions and hypotheses**



# The Polar Front as a major biogeographic boundary in the Southern Ocean

Sections of this chapter have been previously published in Wilkins D., Lauro F. M., Williams T. J., DeMaere M. Z., Brown M. V., Hoffman J. M., Andrews-Pfannkoch C., McQuaid J. B., Riddle M. J., Rintoul S. R., and Cavicchioli R. (2012). Biogeographic partitioning of Southern Ocean picoplankton revealed by metagenomics. *Molecular Ecology*.

## Summary

## Introduction

## Methods

### Sampling and metagenomic sequencing

Sampling<sup>1</sup> was conducted on board the RSV *Aurora Australis* during cruise V3 Collaborative East Antarctic Marine Census/Climate of Southern Ocean (CEAMARC/CASO) from 13 December 2007 – 26 January 2008. This cruise occupied the SR3 latitudinal transect from Hobart, Australia (44° S) to the Mertz Glacier, Antarctica (67° S) within a longitudinal range of 140–150° E. Nineteen samples (16 surface, 3 deep) were obtained along almost the entire latitudinal range (Figure 1).

A range of data were recorded by integrated instruments on the RSV *Aurora Australis* including location, water column depth, water temperature, salinity, fluorescence and meteorological data (Table 1).

---

<sup>1</sup>Sampling was performed by Jeffrey M. Hoffman and Jeffrey B. McQuaid

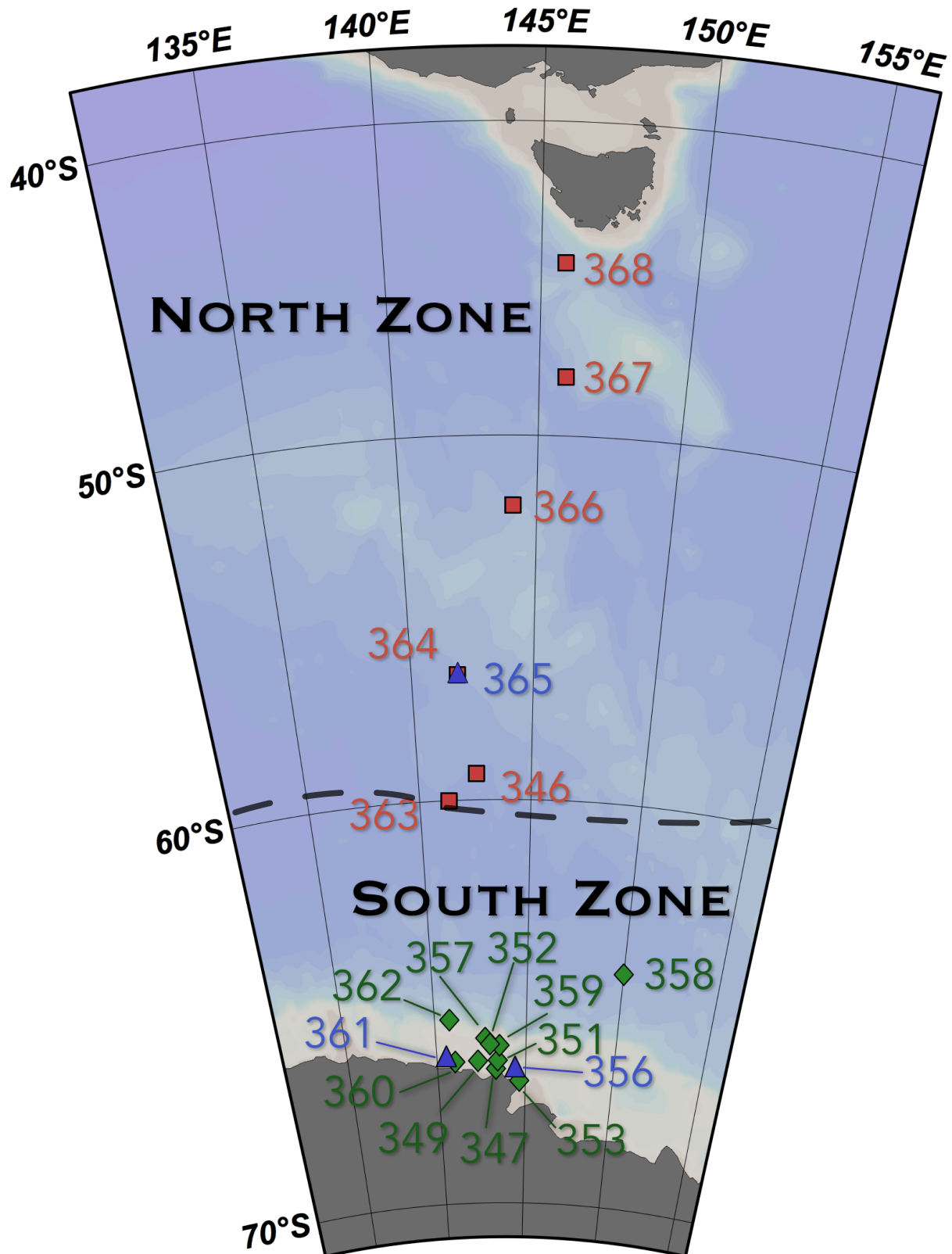


Figure 1: Sites of seawater samples used in this study. Red squares indicate surface samples from the North Zone; green diamonds samples from the South Zone; and blue triangles indicate deep samples. The dashed line gives the approximate location of the Polar Front.

These data were used to locate the Polar Frontal Zone (PFZ) based on a surface temperature gradient of  $\sim 1.35$  °C across a distance of 45–65 km, placing the Polar Front (PF) at approximately  $-59.70^\circ$  of latitude, consistant with previous descriptions (Moore *et al.*, 1999; Sokolov and Rintoul, 2002). Samples were accordingly grouped into “North” and “South” zones, while the three deep samples composed a “Deep” zone (Table 1). The North Zone (NZ) represents waters from the Subtropical, Subantarctic and PFZ regions, while the South Zone (SZ) represents the Antarctic Zone (AZ).

At each station,  $\sim 250$ – $560$  L of seawater was pumped from  $\sim 1.5$ – $2.5$  m below the sea surface into drums stored at ambient temperature on deck. In the case of deep samples,  $\sim 225$ – $230$  L of seawater was collected from Niskin bottles attached to a CTD (SeaBird, Bellevue, USA). Seawater samples were prefiltered through a 20  $\mu\text{m}$  plankton net, then filtrate was captured on sequential 3.0  $\mu\text{m}$  0.8  $\mu\text{m}$  and 0.1  $\mu\text{m}$  293 mm polyethersulfone membrane filters (Port Washington, USA), and immediately stored at  $-20$  °C (Rusch *et al.*, 2007; Ng *et al.*, 2010).

DNA extraction<sup>2</sup> was performed at the J. Craig Venter Institute (Rockville, USA) as described in Rusch *et al.* (2007). Pyrosequencing was performed on a GS20 FLX Titanium instrument (Roche, Branford, USA) also at the J. Craig Venter Institute as described in Lauro *et al.* (2011). Duplicate reads and reads with many pyrosequencing errors were removed as described in Lauro *et al.* (2011).

## Phylogenetic analysis of metagenomic data

### BLAST comparison to RefSeq database

A subset of the RefSeq microbial (bacterial and archaeal) genome database (release 41, retrieved May 31 2012 from <ftp://ftp.ncbi.nih.gov/refseq/release/>) was prepared by excluding sequences with the words “shotgun”, “contig”, “partial”, “end” or “part” in their headers (Angly *et al.*, 2009). Because this database was not expected to contain representative genomes for every species present, OTUs in this study are defined by the best species match to this database, and may for example represent congeners.

The metagenomic reads from each sample were compared against this database using TBLASTX, with default parameters except for: E-value threshold  $1.0 \times 10^{-3}$ , cost to open gap 11, cost to extend gap 1, masking of query sequence by SEG masking with lookup table only. The outputs of all TBLASTX searches against RefSeq were processed by MINSPEC (see section following), and hits not belonging to the minimal sets were removed.

---

<sup>2</sup>DNA extraction was performed by Cynthia Andrews-Pfannkoch and others at the J. Craig Venter Institute

Table 1: Sampling time, location and physiochemical properties of samples used in this study. All data were retrieved from underway instruments aboard the RSV *Aurora Australis*, with the exception of temperature, salinity and fluorescence data for the three deep samples, which was obtained from the CTD (SeaBird, Bellevue, USA) instrument used to collect the samples.

Sample	Zone	Date	Latitude	Longitude	Water Column Depth (m)	Sample Depth (m)	Temperature (°C)	Salinity (PSU)	Fluorescence ( $\mu\text{g L}^{-1}$ )	Volume filtered (L)
346	North	20/12/07	-59.3120	142.5949	4294	2	2.9	33.75	0.3	500
347	South	23/12/07	-66.0213	142.7380	450	2	0.6	34.20	4.0	250
349	South	27/12/07	-66.5662	142.3169	370	1.5	-1.3	34.40	2.3	250
351	South	28/12/07	-66.5587	143.4303	823	1.5	-0.6	34.30	1.3	500
352	South	29/12/07	-66.7650	143.3240	164	2.5	-0.8	34.30	3.1	500
353	South	30/12/07	-67.0521	144.6786	180	2	-1.8	34.40	0.3	500
356	Deep	03/01/08	-66.7617	144.4138	920	920	-1.9	34.69	0.1	230
357	South	05/01/08	-66.1719	143.0193	580	2	-0.4	34.15	2.5	500
358	South	09/01/08	-64.3001	150.0306	3550	2	0	33.55	0.5	500
359	South	12/01/08	-66.1903	143.5292	540	2	-0.2	34.21	2.5	500
360	South	13/01/08	-66.5817	141.0211	316	2	-0.7	34.04	6.2	500
361	Deep	14/01/08	-66.4727	140.5572	1203	1170	-1.8	34.56	0.1	225
362	South	19/01/08	-65.5367	140.8287	1064	2	0.7	32.20	0.5	500
363	North	22/01/08	-60.0001	141.3094	4473	2	3.3	33.77	0.1	500
364	North	23/01/08	-56.6953	141.8780	3693	2	4	33.70	0.5	500
365	Deep	23/01/08	-56.6967	141.9125	3693	3693	0.5	34.69	0.1	230
366	North	24/01/08	-52.0233	144.1362	3180	2	7.6	33.84	0.3	500
367	North	25/01/08	-48.2487	145.9025	3490	2	11	34.43	0.2	500
368	North	26/01/08	-44.7180	145.7775	3201	2	14.8	34.96	1.3	560

## **Identification of minimal species sets with MINSPEC**

A computational method to minimise false OTU identifications and increase the accuracy of OTU abundance estimates (MINSPEC) was developed and implemented in PERL<sup>3</sup>. Following the approach of Ye and Doak (2009) to the parsimonious reconstruction of biochemical pathways (MINPATH), MINSPEC computes the smallest set of OTUs sufficient to explain a set of observed high-quality hits against RefSeq (or any other sequence database). The minimal set computation is framed as a linear programming problem and solved with the GNU Linear Programming Toolkit (GLPK) tool GLPK LINEAR PROGRAMMING/MIP SOLVER (GLPSOL) (Free Software Foundation, Boston). This approach eliminates many of the spurious OTU identifications which result from reads with strong identity to more than one OTU. The “minimal species set” is liable to exclude some low-abundance OTUs, but gives more faithful abundance estimates and eliminates many false positives.

To validate this approach and estimate error rates, simulated microbial assemblages were generated and simulated metagenomic sampling and BLAST search was performed on each assemblage. To simulate sequence identity between taxa, each simulated taxon went through up to fifty rounds in which another taxon was selected at random and deemed to have sequence identity with the first. After each round, the this process was terminated with a 10% probability to simulate an exponential curve of interrelatedness between taxa. A random subset of the simulated taxa were then selected to form the simulated assemblage. This allowed for the possibility of taxa in the assemblage having “sequence identity” to taxa outside it, thus representing the problem MINSPEC was designed to mitigate. A simulated BLAST search was then performed, in which a taxon was selected at random to generate a BLAST hit. To represent a lack of species evenness, taxa were more or less likely to produce a hit according to a logarithmic relationship with their rank within the assemblage, producing a naturalistic rank-abundance curve. Each time a taxon was selected to produce a hit, other taxa with simulated sequence identidy were also selected to produce hits for that “read”, again simulating the problem of a single read producing multiple hits to closely related taxa.

To fully explore the limits and reliability of MINSPEC, the simulated metagenomic experiment described above was performed with all possible permutations of the following parameters: number of simulated taxa [100, 1000, 10000, 50000, 100000]; size of simulated assemblage [1, 10, 100, 300, 500, 1000, 10000]; number of simulated metagenomic reads [10, 100, 1000, 10000, 100000, 200000]. Each permutation was repeated five times, except for those where the size of the assemblage would exceed the number of taxa simulated. The resulting simulated BLAST outputs were processed with MINSPEC, and the false positive (percentage of taxa not in the assemblage which nevertheless survived MINSPEC

---

<sup>3</sup>MINSPEC and the associated metagenomic simulation and validation scripts are open source and available at <https://github.com/wilcox/minspec>; a copy has also been provided in the supplementary information.

filtering) and false negative (percentage of taxa present in the assemblage which were not present after minspecl filtering) rates calculated. Because a high false negative rate can arise from undersampling, a problem in metagenomic studies both real and simulated, an additional “false negative (MINSPEC)” metric was calculated, which excluded taxa which were present in the assemblage but through random chance did not generate any reads, the equivalent of “unsampled rare taxa”. This rate thus represented only false negatives attributable to MINSPEC itself. Finally, as a measure of MINSPEC’s usefulness, the proportion of “false” taxa — those which generated BLAST hits but were not part of the assemblage — that were successfully removed by MINSPEC was calculated.

### OTU abundances and variance between zones

The relative OTU abundances for each sample were determined using the PERL script Genome relative Abundance and Average Size (GAAS) (Angly *et al.*, 2009). Briefly, GAAS estimates the relative abundance of OTUs from the number and quality of BLAST hits to each species, taking into account differences in genome size. GAAS was run with the default settings. To normalise for reads which did not yield acceptable hits, the relative abundances for each sample were scaled by that sample’s effective BLAST hit rate. An OTU profile was generated for each sample by encoding the scaled relative abundance of each OTU from each size fraction as a separate variable.

To test the hypothesis that the oceanic zones harbour significantly different communities, Analysis of SIMilarities (ANOSIM) with 999 permutations was performed on a standardised, log-transformed Bray-Curtis resemblance matrix of OTU profiles. SIMilarity PERcentages (SIMPER) analysis was performed to identify the contribution of individual OTUs to differences between the zones. All statistical procedures were performed in PRIMER 6 as described by Clarke and Warwick (2001).

### Functional analysis of metagenomic data

#### BLAST comparison to Kyoto Encyclopedia of Genes and Genomes (KEGG) database

In order to identify functional differences between the zones, the set of metagenomic reads from each sample was compared against the KEGG GENES database (retrieved July 2 2010 from <ftp://ftp.genome.jp/pub/kegg/genes/fasta/genes.pep>) with BLASTX, with default parameters except for: maximum number of database sequence alignments 10; E-value threshold  $1.0 \times 10^{-3}$ ; gap opening penalty 11; gap extension penalty 1; masking of query sequence by SEG masking for lookup table only.

## Analysis of functional potential

Genes identified by BLASTX were aggregated to KEGG ortholog groups according to the KEGG Orthology schema (<ftp://ftp.genome.jp/pub/kegg/genes/ko>, retrieved Mar 29 2011), and ortholog group abundances calculated for each sample. Following Coleman and Chisholm (2010), a read was considered a hit to a given ortholog group if the top three hits for that read (or all hits if fewer than three total hits) were to genes from the same ortholog group, and had bit scores > 40. If the bit score difference between any two top hits was greater than 30, only the hits above this difference were considered.

Ortholog group counts were then used to calculate the abundance of KEGG modules. Because many ortholog groups are members of more than one module, the abundance  $a_m$  of each module  $m$  was calculated as

$$a_m = \sum_{K=1}^n \frac{C_K}{M_K}$$

where  $n$  is the number of ortholog groups  $K$  belonging to module  $m$ ,  $C_K$  is the number of hits to ortholog group  $K$ , and  $M_K$  is the total number of modules to which  $K$  belongs. To account for differences in sequencing depth between samples, module abundances were scaled to 500,000 reads per sample. To test the hypothesis that the NZ and SZ harbour significantly different functional potential, one-way ANOSIM with 999 permutations was performed as above on a standardised, log-transformed Bray-Curtis distance resemblance matrix of the module and ortholog group profiles. A functional profile was generated for each sample by summing the scaled abundances of each module from all size fractions, and SIMPER performed as above to identify modules which contributed highly to the variation in functional potential between the two zones. Modules with a high contribution to variance or otherwise of interest were then linked to taxonomy (“taxonomic decomposition”) by noting the genus of the organism associated with each gene in the KEGG GENES database and thus calculating the relative contribution of each genus to each module’s abundance. This allowed functional contributions to be putatively assigned to genera which were not identified in our taxonomic analysis, as the database included gene sequences for organisms for which a full genome was not available.

## Results

### Metagenomic sequencing

6.6 Gbp of 454 sequence data representing picoplankton in the size range 0.1 – 3.0 µm was obtained from 16 samples. After removal of low-quality reads, 454 sequencing yielded 157,507 – 597,689 reads per sample (mean 354,399) of lengths ranging from 100 to 606 bp (mean 378).

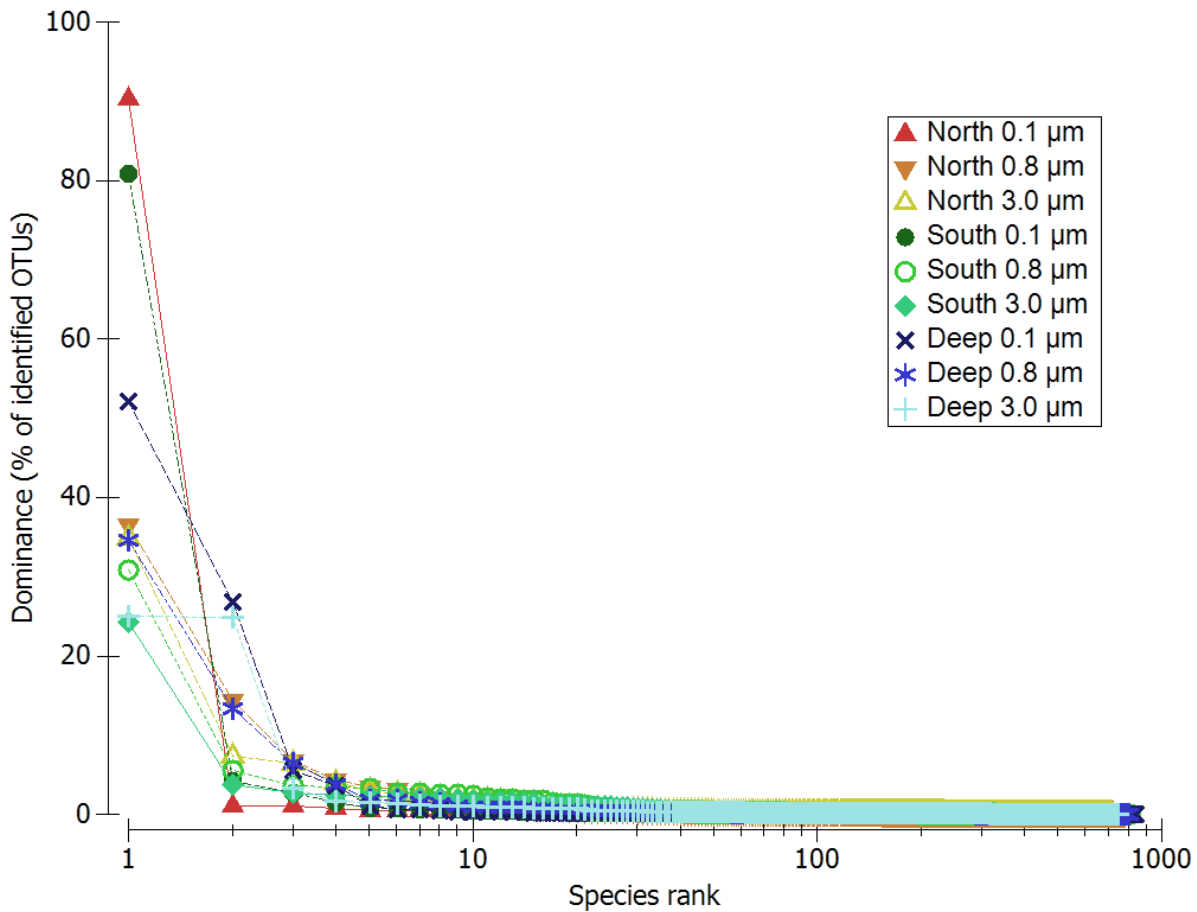


Figure 2: Rank-abundance curves for OTUs identified in each zone and size fraction. The dominance of a given OTU is its relative abundance as a percentage of all identified OTUs. The x-axis is scaled logarithmically. Generated using PRIMER 6.

### Phylogenetic analysis of metagenomic data

The proportion of reads in each sample which yielded matches to RefSeq ranged from 25% to 85% (mean 62%). The most abundant OTUs in each sample are given in Table 2 and a full list of OTU abundances in the supplementary material (PF-all-OTUs.csv). All samples and size fractions exhibited very low OTU evenness (Figure 2).

ANOSIM analysis showed that the zones harbor significantly different microbial communities ( $R = 0.451$ ,  $p < 0.004$ ). SIMPER was performed in order to identify the contribution of individual OTUs to the difference between the NZ and SZ. The results for the highest contributors are provided in Table 3, and are graphically summarised for all OTUs in Figure 3.

The SIMPER analysis found that no single OTU contributed more than 2.9% of variance and 74% of variance was contributed by OTUs with a contribution less than 1%. There was also a large difference in the contribution to variance of the three size fractions, with approximately 52% of all variance contributed by OTUs from the 3.0  $\mu\text{m}$  fraction, 37% by the 0.8  $\mu\text{m}$  fraction, and 9% by the 0.1  $\mu\text{m}$

Table 2: Relative abundances (as percentages) of the twenty most abundant OTUs identified in this study, in each zone and size fraction.

	North					South					Deep		
	0.1 µm	0.8 µm	3.0 µm	0.1 µm	0.8 µm	3.0 µm	0.1 µm	0.8 µm	3.0 µm	0.1 µm	0.8 µm	3.0 µm	
<i>Pelagibacter ubique</i> HTCC1062	61.76	25.00	23.87	58.85	22.40	17.61	37.05	24.56	17.66				
<i>Nitrosopumilus maritimus</i> SCM1	0.01996	0.01438	0.009508	1.076	1.309	1.210	19.09	9.463	17.77				
<i>Ruthia magnifica</i> str. Cm ( <i>Calyptogena magnifica</i> )	0.6699	0.6458	0.5484	2.987	2.616	1.025	3.945	4.601	2.264				
<i>Roseobacter</i> sp. OCh114	0.3125	2.932	1.588	0.4477	3.994	2.657	0.1259	1.228	0.6792				
<i>Synechococcus</i> sp. CC9902	0.1081	9.837	4.973	0.0007484	0.004156	0.09733	0.002846	0.01502	0.01058				
<i>Silicibacter pomeroyi</i> DSS-3	0.2578	2.286	1.154	0.3070	2.505	1.576	0.1224	0.9417	0.4988				
<i>Gramella forsetii</i> strain KT0803	0.2412	1.210	1.755	0.4993	2.347	1.890	0.2078	0.6179	0.5173				
<i>Candidatus Vesicomyosococcus okutanii</i> strain HA	0.4634	0.4642	0.2078	1.970	1.807	0.2174	2.480	2.662	1.167				
<i>Robiginitalea biflormata</i> strain HTCC2501	0.2751	1.099	1.297	0.4722	1.878	1.405	0.2265	0.6188	0.6946				
<i>Flavobacterium psychrophilum</i> strain JIP02/86	0.1718	0.8409	1.224	0.4316	1.960	1.598	0.1599	0.4744	0.6001				
<i>Synechococcus</i> sp. CC9311	0.03014	4.624	4.409	0.0007221	0.002778	0.02764	0.001580	0.002863	0.009241				
<i>Candidatus Puriceipirillum marinum</i> IMCC1322	0.6444	2.077	1.267	0.3586	1.377	0.7109	0.3425	1.062	0.5345				
<i>Silicibacter</i> sp. TM1040	0.2274	1.652	0.8738	0.2709	1.803	1.233	0.07665	0.5890	0.2957				
<i>Jannaschia</i> sp. DFL-12	0.1776	1.378	0.7350	0.2443	1.692	0.8009	0.07338	0.6515	0.3078				
<i>Zunongwangia profunda</i> strain SM-A87	0.1522	0.7487	1.059	0.2968	1.410	1.204	0.1353	0.3478	0.4971				
<i>Colwellia</i> sp. 34H	0.02345	0.3636	2.736	0.05207	0.5140	1.041	0.05137	0.4687	0.8013				
<i>Coralliomargarita akajimensis</i> strain DSM 45221	0.03698	0.07573	0.1197	0.1154	1.543	1.680	0.02614	0.3040	0.2740				
<i>Jannaschina</i> sp. CCS1	0.1173	0.9344	0.4784	0.1711	1.230	0.8239	0.05865	0.4462	0.2118				
<i>Pseudalteromonas atlantica</i> strain T6c	0.01251	0.4772	1.993	0.02270	0.4089	1.132	0.02634	0.2143	0.7459				
<i>Saccharophagus degradans</i> strain 2-40	0.06532	0.4325	0.5429	0.1289	1.072	0.8663	0.07798	0.2844	0.3165				
<i>Flavobacterium johnsoniae</i> strain UW101	0.08822	0.4220	0.6141	0.2034	0.9389	0.8578	0.07545	0.2255	0.3300				
<i>Capnocytophaga ochracea</i> strain DSM 7271	0.1143	0.4830	0.5399	0.2314	0.8815	0.6814	0.08964	0.2840	0.5043				
<i>Marinimonas</i> sp. MWYL1	0.03777	0.2529	0.3026	0.1514	1.300	0.7006	0.07393	0.2439	0.2155				
<i>Cellvirobacter japonicus</i> strain Ueda107	0.05884	0.3080	0.3231	0.1155	0.9917	0.4713	0.06774	0.2981	0.2549				
<i>Marinobacter hydrocarbonoclasticus</i> VT8	0.04093	0.2889	0.3883	0.08418	0.7195	0.3848	0.1250	0.6667	1.066				
<i>Pseudalteromonas haloplanktis</i> strain TAC125	0.01389	0.2505	0.8896	0.03427	0.3561	0.6530	0.1092	1.203	0.1503				
<i>Teredinibacter turnerae</i> strain T7901	0.05665	0.3051	0.3081	0.1138	0.9174	0.5127	0.06558	0.2649	0.1885				
<i>Actinobacter baumannii</i> strain SDF	0.004886	0.007187	0.4073	0.006260	0.04218	1.459	0.004285	0.01229	0.3155				

Table 3: The thirty OTUs with the highest contributions to the difference between the NZ and SZ. Abundances are zonal averages and have been standardised and log-transformed. As each OTU on each size fraction was encoded as a separate variable in the SIMPER analysis, the size fraction is given after each OTU name.

OTU	Abundance South	Abundance North	Contribution to variance (%)
<i>Synechococcus</i> sp. CC9311 0.8 µm	0.00	1.08	2.88
<i>Synechococcus</i> sp. CC9902 0.8 µm	0.00	1.04	2.81
<i>Synechococcus</i> sp. CC9311 3.0 µm	0.01	0.98	2.59
<i>Synechococcus</i> sp. CC9902 3.0 µm	0.04	0.76	2.03
<i>Pelagibacter ubique</i> HTCC1062 3.0 µm	1.97	2.40	1.97
<i>Ruthia magnifica</i> str. Cm ( <i>Calyptogena magnifica</i> ) 0.1 µm	0.82	0.25	1.57
<i>Colwellia</i> sp. 34H 3.0 µm	0.34	0.66	1.32
<i>Ruthia magnifica</i> str. Cm ( <i>Calyptogena magnifica</i> ) 0.8 µm	0.74	0.25	1.32
<i>Pelagibacter ubique</i> HTCC1062 0.8 µm	2.32	2.48	1.32
<i>Candidatus Vesicomyosocius okutanii</i> strain HA 0.1 µm	0.62	0.18	1.20
<i>Coraliomargarita akajimensis</i> strain DSM 45221 0.8 µm	0.48	0.04	1.13
<i>Coraliomargarita akajimensis</i> strain DSM 45221 3.0 µm	0.49	0.06	1.10
<i>Roseobacter</i> sp. OCh114 0.8 µm	1.01	0.81	1.08
<i>Pseudoalteromonas atlantica</i> strain T6c 3.0 µm	0.38	0.54	1.08
<i>Candidatus Vesicomyosocius okutanii</i> strain HA 0.8 µm	0.57	0.19	1.04
<i>Acinetobacter baumannii</i> strain SDF 3.0 µm	0.45	0.18	0.95
<i>Gramella forsetii</i> strain KT0803 0.8 µm	0.72	0.43	0.94
<i>Marinomonas</i> sp. MWYL1 0.8 µm	0.46	0.11	0.92
<i>Roseobacter</i> sp. OCh114 3.0 µm	0.76	0.54	0.91
<i>Flavobacterium psychrophilum</i> strain JIP02/86 0.8 µm	0.63	0.32	0.89
<i>Silicibacter pomeroyi</i> DSS-3 0.8 µm	0.75	0.69	0.86
<i>Brachyspira hyodysenteriae</i> strain WA1 3.0 µm	0.47	0.19	0.84
<i>Ruthia magnifica</i> str. Cm ( <i>Calyptogena magnifica</i> ) 3.0 µm	0.34	0.21	0.82
<i>Pseudoalteromonas haloplanktis</i> strain TAC125 3.0 µm	0.22	0.33	0.77
<i>Robiginitalea bifomata</i> strain HTCC2501 0.8 µm	0.61	0.40	0.74
<i>Nitrosopumilus maritimus</i> SCM1 0.1 µm	0.27	0.01	0.72
<i>Gramella forsetii</i> strain KT0803 3.0 µm	0.59	0.59	0.71
<i>Lysinibacillus sphaericus</i> strain C3-41 3.0 µm	0.29	0.02	0.71
<i>Nitrosopumilus maritimus</i> SCM1 0.8 µm	0.25	0.01	0.70
<i>Silicibacter</i> sp. TM1040 0.8 µm	0.59	0.55	0.69

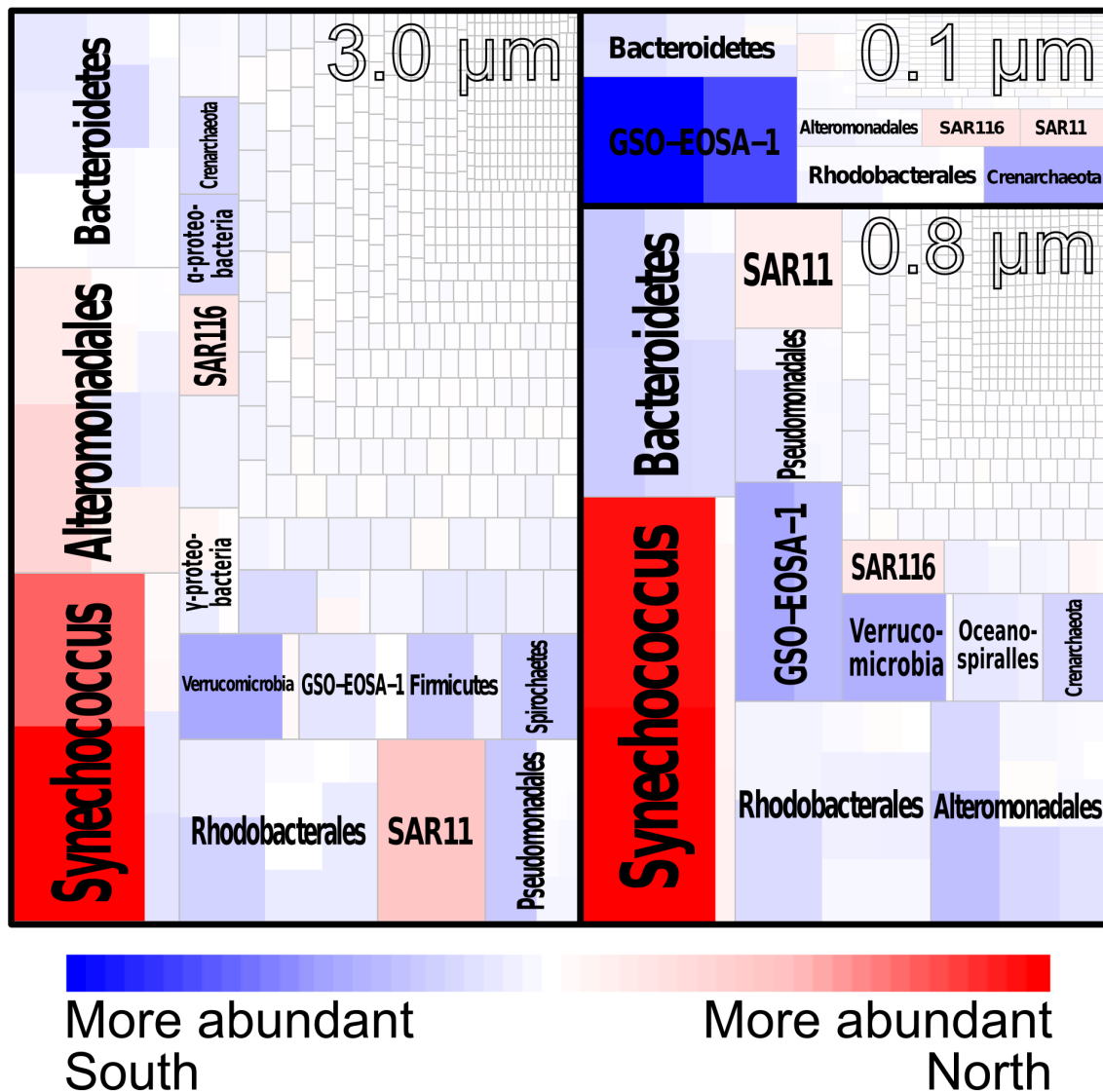


Figure 3: Contribution of OTUs to variance between the North and South zones, and differential abundance of OTUs from each size fraction between the two zones. Each coloured (red or blue) rectangle represents an OTU identified through analysis of BLAST matches between SO metagenome data and the RefSeq database. The area of each rectangle as a proportion of the total plot area corresponds to that OTU's contribution to the total variance between the two zones. The colour of each rectangle corresponds to difference in relative abundance of that OTU between the zones, with blue indicating a higher relative abundance south of the PF, and red a higher abundance north of the PF. OTUs from clades or taxonomic ranks of interest have been grouped, with labels in bold and groups separated by gray lines. Groups and OTUs with a low contribution to variance which were not grouped are unlabeled. OTUs from each size fraction have also been grouped, with labels in black outline and size fractions separated by thick black lines. The total contribution to variance of each size fraction is given as a percentage. The data used to generate this figure are given in the supplementary material (PF-OTUs-SIMPER.csv).

fraction. Notably, OTUs within several taxonomic groups that had high contribution to variance covaried in their relative representation in the NZ and SZ. For example, Bacteroidetes and GSO-EOSA-1 representatives were on average more abundant in the SZ; while *Prochlorococcus* and *Synechococcus* spp., SAR11 and SAR116 were on average more abundant in the NZ (Figure 3). Some groups, such as the Alteromonadales, had variable relative representation depending on size fraction.

#### **Validation of MINSPEC**

TODO working on this section Here is a ref to the figure (Figure 4). And for fun, the false positives only (Figure 4b).

#### **Functional analysis of metagenomic data**

TODO working on this section

ANOSIM analysis of the samples' KEGG ortholog group and module profiles revealed that the zones had significantly different functional potential (ortholog group:  $R = 0.642$ ,  $p < 0.001$ ; module:  $R = 0.871$ ,  $p < 0.001$ ). SIMPER was performed on the profiles in order to identify the specific functional differences between the zones. The highest-contributing modules are given in Table 4, and a complete list in the supplementary material (PF-modules-SIMPER.csv). The highest-contributing ortholog groups are given in Table 5, and a complete list in the supplementary material (PF-ortholog-groups-SIMPER.csv). No single ortholog group or module contributed more than 2.2% of the variance, indicating a complex and diverse pattern of functional differences. There was a strong trend for ortholog groups and modules with higher contributions to variance to be overrepresented in the NZ in the 3.0  $\mu\text{m}$  fraction but the SZ in the smaller fractions, indicating that the functional diversity of each zone was strongly segregated by size fraction.

## **Discussion**

## **Conclusions**

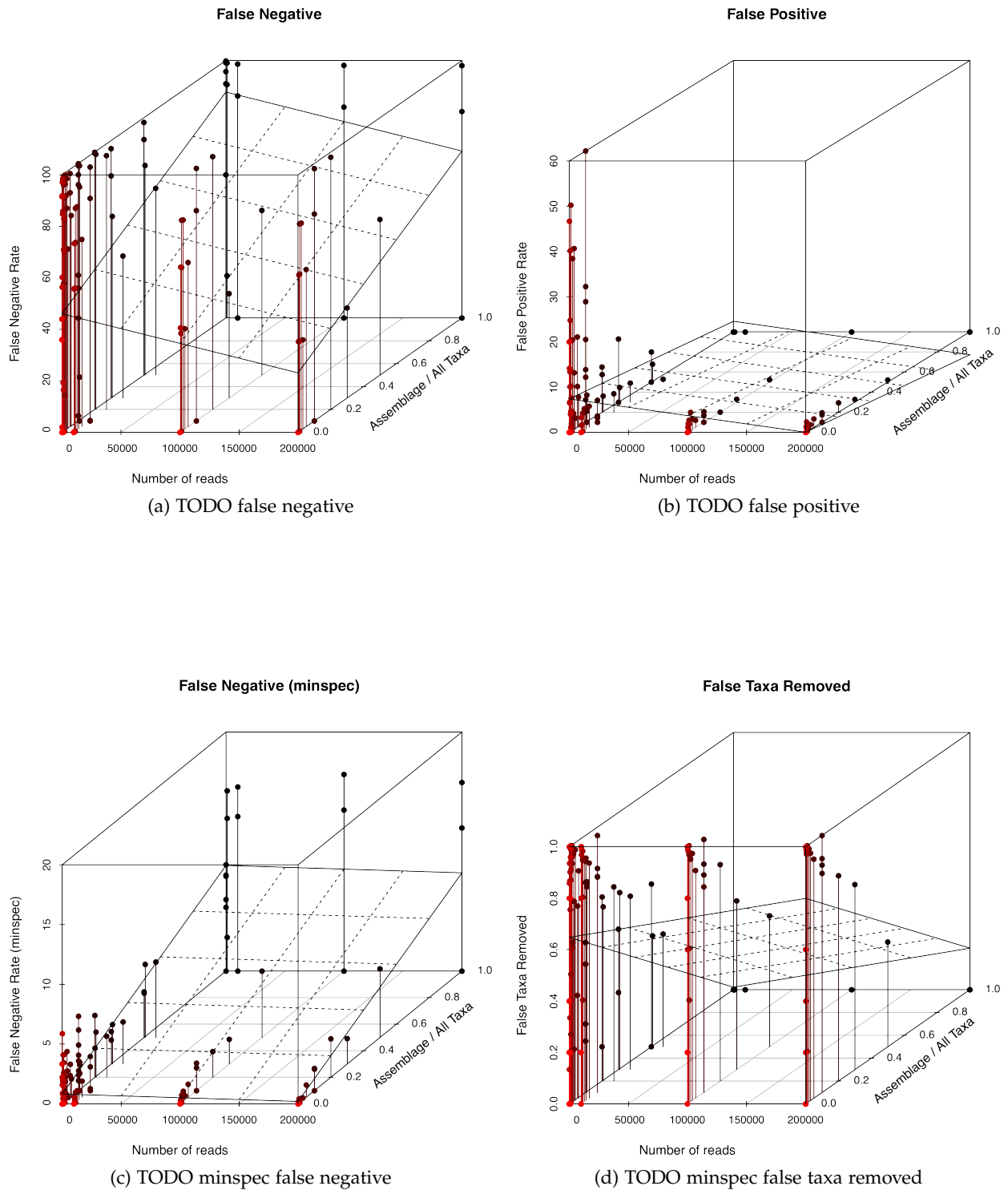


Figure 4: TODO master caption

Table 4: The thirty KEGG modules with the highest contributions to the difference between the NZ and SZ. Abundances are zonal averages and have been standardised and log-transformed.

KEGG module	Abundance South	Abundance North	Contribution to variance (%)
Photosystem II	0.42	0.57	2.21
Complex I (NADH dehydrogenase), NADH dehydrogenase I/diaphorase subunit of the bidirectional hydrogenase	0.01	0.24	1.80
Photosystem I	0.43	0.34	1.70
Pyrimidine deoxyribonucleotide biosynthesis, CDP/CTP → dCDP/dCTP,dTDP/dTTP	0.51	0.66	1.16
Histidine degradation, histidine → N-formiminoglutamate → glutamate	0.42	0.31	1.14
Methionine salvage pathway	0.29	0.43	1.14
sn-Glycerol 3-phosphate transport system	0.29	0.16	1.11
Complex I (NADH dehydrogenase), NADH dehydrogenase I	1.08	1.05	1.06
Branched-chain amino acid transport system	0.79	0.83	0.96
Dipeptide transport system	0.14	0.02	0.95
Adenine nucleotide biosynthesis, IMP → ADP/dADP,ATP/dATP	0.62	0.74	0.95
Glycine betaine/proline transport system	0.66	0.56	0.94
Sulfur reduction, sulfate → H <sub>2</sub> S	0.54	0.44	0.91
Simple sugar transport system	0.46	0.39	0.90
Peptides/nickel transport system	0.99	0.98	0.89
Ribosome, eukaryotes	0.26	0.27	0.89
Multiple sugar transport system	0.55	0.55	0.86
Type II general secretion system	0.21	0.21	0.82
Sulfonate/nitrate/taurine transport system	0.45	0.37	0.82
Guanine nucleotide biosynthesis, IMP → GDP/dGDP,GTP/dGTP	0.72	0.82	0.81
RNA polymerase II, eukaryotes	0.11	0.20	0.76
Histidine biosynthesis, PRPP → histidine	0.94	0.86	0.76
Putrescine transport system	0.18	0.09	0.72
Leucine biosynthesis, pyruvate → 2-oxoisovalerate → leucine	1.29	1.37	0.71
C <sub>5</sub> isoprenoid biosynthesis, non-mevalonate pathway	0.70	0.77	0.71
Leucine degradation, leucine → acetoacetate + acetyl-CoA	0.64	0.59	0.71
Thiamine transport system	0.13	0.05	0.69
Spliceosome, 35S U5-snRNP	0.18	0.20	0.68
Cytochrome b <sub>6f</sub> complex	0.14	0.12	0.67
Menaquinone biosynthesis, chorismate → menaquinone	0.25	0.27	0.66

Table 5: The thirty KEGG ortholog groups with the highest contribution to the difference between the NZ and SZ. Abundances are zonal averages and have been standardised and log-transformed. As each ortholog group on each size fraction was encoded as a separate variable in the SIMPER analysis, the size fraction is given after each ortholog group name.

OTU		Abundance South	Abundance North	Contribution to variance (%)
Hypothetical protein 3.0 $\mu\text{m}$		0.11	0.24	0.26
Hypothetical protein 0.8 $\mu\text{m}$		0.68	0.57	0.24
Ribonucleoside-diphosphate reductase alpha chain [EC:1.17.4.1] 0.8 $\mu\text{m}$		0.17	0.24	0.15
DNA polymerase III subunit alpha [EC:2.7.7] 0.8 $\mu\text{m}$		0.25	0.19	0.14
Hypothetical protein 0.1 $\mu\text{m}$		0.26	0.24	0.12
Proline dehydrogenase / delta 1-pyrroline-5-carboxylate 0.8 $\mu\text{m}$		0.10	0.04	0.12
Aminomethyltransferase [EC:2.1.2.10] 0.8 $\mu\text{m}$		0.25	0.19	0.12
Ribonucleoside-diphosphate reductase alpha chain [EC:1.17.4.1] 3.0 $\mu\text{m}$		0.02	0.08	0.12
Sarcosine oxidase, subunit alpha [EC:1.5.3.1] 0.8 $\mu\text{m}$		0.22	0.17	0.12
Integrator complex subunit 6 3.0 $\mu\text{m}$		0.07	0.05	0.11
Multicomponent $\text{Na}^+:\text{H}^+$ antiporter subunit D 0.8 $\mu\text{m}$		0.11	0.05	0.11
Glutamine synthetase [EC:6.3.1.2] 0.8 $\mu\text{m}$		0.24	0.19	0.11
Pyruvate dehydrogenase E1 component [EC:1.2.4.1] 0.8 $\mu\text{m}$		0.15	0.10	0.11
Cobaltochelatase CobN [EC:6.6.1.2] 0.8 $\mu\text{m}$		0.11	0.06	0.11
Formate dehydrogenase, alpha subunit [EC:1.2.1.2] 0.8 $\mu\text{m}$		0.15	0.10	0.11
DNA-directed RNA polymerase subunit beta [EC:2.7.7.6] 3.0 $\mu\text{m}$		0.03	0.08	0.11
Glutamate synthase (NADPH/NADH) large chain [EC:1.4.1.13 1.4.1.14] 0.8 $\mu\text{m}$		0.25	0.22	0.11
Dimethylglycine dehydrogenase [EC:1.5.99.2] 0.8 $\mu\text{m}$		0.17	0.14	0.11
Flagellin 0.8 $\mu\text{m}$		0.06	0.10	0.10
DNA-directed RNA polymerase subunit beta [EC:2.7.7.6] 3.0 $\mu\text{m}^a$		0.03	0.08	0.10
Photosystem II PsbA protein 0.8 $\mu\text{m}$		0.01	0.06	0.09
Aldehyde dehydrogenase (NAD+) [EC:1.2.1.3] 0.8 $\mu\text{m}$		0.17	0.13	0.09
Glutamate synthase (NADPH/NADH) large chain [EC:1.4.1.13 1.4.1.14] 3.0 $\mu\text{m}$		0.02	0.07	0.09
Thymidylylate synthase (FAD) [EC:2.1.1.148] 0.8 $\mu\text{m}$		0.02	0.06	0.09
Topoisomerase IV subunit A [EC:5.99.1.-] 0.8 $\mu\text{m}$		0.11	0.07	0.09
DNA mismatch repair protein MutS 0.8 $\mu\text{m}$		0.13	0.08	0.09
Glutamate dehydrogenase [EC:1.4.1.2] 0.8 $\mu\text{m}$		0.07	0.03	0.09
DNA polymerase I [EC:2.7.7] 0.1 $\mu\text{m}$		0.12	0.11	0.09
GTP-binding protein 0.8 $\mu\text{m}$		0.26	0.21	0.09
GTP-binding protein 3.0 $\mu\text{m}$		0.03	0.07	0.09

<sup>a</sup>Due to an error in the KEGG database, this module is encoded twice.



# **Meso-scale biogeographic drivers of planktonic diversity**



# **Conclusions**



# References

- Angly F. E., Willner D., Prieto-Davó A., Edwards R. A., Schmieder R., Vega-Thurber R., Antonopoulos D. A., Barott K., Cottrell M. T., Desnues C., Dinsdale E. A., Furlan M., Haynes M., Henn M. R., Hu Y., Kirchman D. L., McDole T., McPherson J. D., Meyer F., Miller R. M., Mundt E., Naviaux R. K., Rodriguez-Mueller B., Stevens R., Wegley L., Zhang L., Zhu B., and Rohwer F. (2009). The GAAS Metagenomic Tool and Its Estimations of Viral and Microbial Average Genome Size in Four Major Biomes. *PLoS Computational Biology*, 5(12):e1000593.
- Clarke K. R. and Warwick R. M. *Changes in marine communities: an approach to statistical analysis and interpretation*. PRIMER-E, Plymouth, 2nd edition, 2001.
- Coleman M. L. M. and Chisholm S. W. S. (2010). Ecosystem-specific selection pressures revealed through comparative population genomics. *Audio, Transactions of the IRE Professional Group on*, 107(43):18634–18639.
- Lauro F. M., DeMaere M. Z., Yau S., Brown M. V., Ng C., Wilkins D., Raftery M. J., Gibson J. A., Andrews-Pfannkoch C., Lewis M., Hoffman J. M., Thomas T., and Cavicchioli R. (2011). An integrative study of a meromictic lake ecosystem in Antarctica. *The ISME journal*, 5(5):879–895.
- Moore J. K., Abbott M. R., and Richman J. G. (1999). Location and dynamics of the Antarctic Polar Front from satellite sea surface temperature data. *Journal of Geophysical Research*, 104:3052–3073.
- Ng C., DeMaere M. Z., Williams T. J., Lauro F. M., Raftery M., Gibson J. A., Andrews-Pfannkoch C., Lewis M., Hoffman J. M., Thomas T., and Cavicchioli R. (2010). Metaproteogenomic analysis of a dominant green sulfur bacterium from Ace Lake, Antarctica. *The ISME journal*, 4(8):1002–1019.
- Rusch D. B., Halpern A. L., Sutton G., Heidelberg K. B., Williamson S., Yooseph S., Wu D., Eisen J. A., Hoffman J. M., Remington K., Beeson K., Tran B., Smith H., Baden-Tillson H., Stewart C., Thorpe J., Freeman J., Andrews-Pfannkoch C., Venter J. E., Li K., Kravitz S., Heidelberg J. F., Utterback T., Rogers Y.-H., Falcón L. I., Souza V., Bonilla-Rosso G., Eguiarte L. E., Karl D. M., Sathyendranath S., Platt T., Bermingham E., Gallardo V., Tamayo-Castillo G., Ferrari M. R., Strausberg R. L., Nealson K., Friedman R., Frazier M., and Venter J. C. (2007). The Sorcerer II Global Ocean Sampling expedition: northwest Atlantic through eastern tropical Pacific. *PLoS Biology*, 5(3):e77–e77.
- Sokolov S. and Rintoul S. R. (2002). Structure of Southern Ocean fronts at 140° E. *Journal of Marine Systems*, 37(1):151–184.
- Wilkins D., Lauro F. M., Williams T. J., DeMaere M. Z., Brown M. V., Hoffman J. M., Andrews-Pfannkoch C., McQuaid J. B., Riddle M. J., Rintoul S. R., and Cavicchioli R. (2012). Biogeographic partitioning of Southern Ocean picoplankton revealed by metagenomics. *Molecular Ecology*.
- Ye Y. and Doak T. G. (2009). A parsimony approach to biological pathway reconstruction/inference for genomes and metagenomes. *PLoS Computational Biology*, 5(8):e1000465.